Chapter 1

ORBITAL EFFECTS IN MANGANITES

Jeroen van den Brink
Computational Materials Science and Mesa$^+$ Institute, Faculty of Applied Physics, University of Twente, P.O. Box 217, 7500 AE Enschede, The Netherlands
jvdb@tn.utwente.nl

Giniyat Khaliullin
Max-Planck-Institut für Festkörperforschung, Heisenbergstr. 1, D-70569 Stuttgart, Germany
G.Khaliullin@fkf.mpg.de

Daniel Khomskii
Laboratory of Applied and Solid State Physics, Materials Science Center, University of Groningen, Nijenborgh 4, 9747 AG Groningen, The Netherlands
khomskii@phys.rug.nl

Abstract We review some aspects related to orbital degrees of freedom in manganites. The Mn^{3+} ions in these compounds have double orbital degeneracy and are strong Jahn-Teller ions, causing structural distortions and orbital ordering. We discuss ordering mechanisms and the consequences of orbital order. The additional degeneracy of low-energy states and the extreme sensitivity of the chemical bonds to the spatial orientation of the orbitals result in a variety of competing interactions. This quite often leads to frustration of classical ordered states and to the enhancement of quantum effects. Quantum fluctuations and related theoretical models are briefly discussed, including the occurence of resonating orbital bonds in the metallic phase of the colossal magnetoresistance manganites.

Keywords: Manganites, orbital order, orbital liquid

Contents

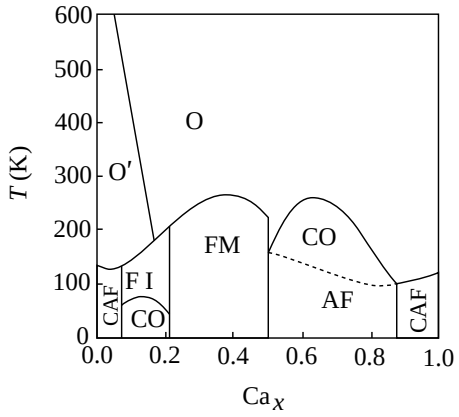

Figure 1.1. Phase diagram of $La_{1-x}Ca_xMnO_3$ (after S.-W. Cheong). O: orthorhombic phase with rotated regular octahedra, O′: orthorhombic phase with Jahn-Teller distortions, CAF: canted antiferromagnet or phase separated state, FI: ferromagnetic insulator, CO: charge order, FM: ferromagnetic metal, AF: antiferromagnet.

1. Introduction

When considering the properties of real systems with strongly correlated electrons, such as transition metal (TM) oxides, one often has to take into account, besides the charge and spin degrees of freedom, described e.g. by the nondegenerate Hubbard model, also the orbital structure of corresponding TM ions. These orbital degrees of freedom are especially important in cases of the so-called orbital degeneracy –the situation when the orbital state of the TM ions in a regular, undistorted coordination (e.g. in a regular O_6-octahedron) turns out to be degenerate [1, 2, 3, 4]. This is e.g. the situation with the ions Cu^{2+} (d^9), Mn^{3+} (d^4), Cr^{2+} (d^4), low-spin Ni^{3+} ($d^7 = t_{2g}^6 e_g^1$). In an isolated centre this degeneracy gives rise to the famous Jahn-Teller effect [5], and in concentrated systems to a cooperative transition which may be viewed as a simultaneous structural phase transition that lifts the orbital degeneracy (cooperative Jahn-Teller transition) and orbital ordering (OO) transition (or quadrupolar ordering transition, a terminology that is often used in rare earth compounds).

All these effects play a very important role in the materials which became very popular recently –in manganites with colossal magnetoresistance (CMR). A typical example is the system $La_{1-x}Ca_xMnO_3$ (there may be other rare earths, e.g. Pr, Nd, or Bi instead of La, or other divalent cations –Sr, Ba, Pb– instead of Ca; there exist also layered materials of this kind). The characteristic phase diagram of these systems is

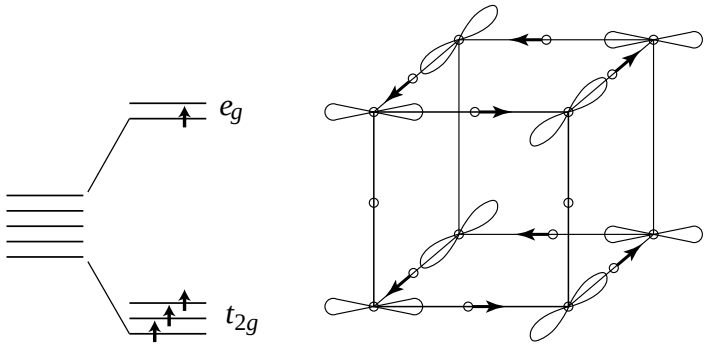

Figure 1.2. Left: splitting of $3d$-levels in a cubic crystal field (regular MnO_6-octahedron). Electron occupation of the four $3d$-electrons in Mn^{3+} is shown by arrows. Right: orbital ordering of $LaMnO_3$. Arrows indicate the displacements of oxygen ions.

shown schematically in Fig. 1.1. The undoped material $LaMnO_3$, which is an antiferromagnetic insulator, contains typical Jahn-Teller ions Mn^{3+} (electronic configuration $t_{2g}^3 e_g^1$) –i.e. it is orbitally doubly-degenerate, see Fig. 1.2. Thus we can expect that the orbital degrees of freedom may significantly influence the properties of CMR manganites –an idea which is largely supported by experiments. In this paper we review some of the aspects of the physics of manganites connected with orbital degrees of freedom. This field is actually already quite large and well developed, and of course we will not be able to cover all of it; much of the material presented will be based on the investigations in which we ourselves participated. Some of the general concepts used below are also presented in [6, 7]. There are a lot of different questions, and a wealth of properities (see the phase diagram in Fig. 1.1) in which orbitals are important. In this chapter we give a general overview of these properties. Most topics we will discuss on a rather qualitative level, trying to explain the main physical effects, but without going into too many details. However, there are some very interesting and important problems in the orbital physics of manganites, which require a more detailed explanation. This, in particular, is the case with genuine quantum effects which may be very important, especially (but not only) in the "optimal doped" ferromagnetic metallic phase. These questions are treated in Section 3 in more detail and on a somewhat more theoretical level.

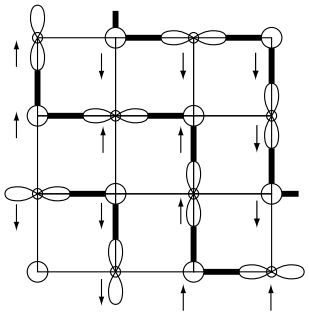

Figure 1.3. Charge, orbital and spin ordering in the basal (xy)-plane of manganates at $x = 0.5$. Arrows denote the spin ordering. The spin zigzags, typical for the CE-type magnetic order, are shown by thick lines.

1.1. Main features of phase diagram: orbital effects

As already mentioned above, the undoped $LaMnO_3$ with the perovskite structure contains strong Jahn-Teller ions Mn^{3+}. They are known to induce a rather strong local distortion in all the insulating compounds that contain them [2]. Also in $LaMnO_3$ it is well known that there exists an orbital ordering and a concomitant lattice distortion: e_g-orbitals of Mn^{3+} ions are ordered in such a way that at the neighbouring Mn sites the alternating $3x^2 - r^2$ and $3y^2 - r^2$-orbitals are occupied, i.e. the local O_6-octahedra are alternatingly elongated along x and y-directions, see Fig. 1.2. Let us mention here the typical energy scales that are involved in the manganites. The ferromagnetic Hunds rule exchange among t_{2g} and e_g-electrons is $J_H \approx 0.8$ eV per spin pair, the crystal field splitting between these levels (see Fig. 1.2) is $10Dq \approx 2 - 3$ eV, and the Jahn Teller energy, E_{JT}, which is the splitting of the e_g-states by the lattice distortion, is typically an order of magnitude smaller than $10Dq$.

Orbital ordering is also known to exist in most manganites in another well-defined region of the phase diagram –at half-doping $x = 0.5$. In this situation with decreasing temperature charge ordering –the checkerboard arrangement of Mn^{3+} and Mn^{4+} ions in the basal plane, see Fig. 1.3 [1, 8, 9] – sets in. The Mn^{3+}-ions with localized electrons again have an orbital degeneracy (Mn^{4+} (t_{2g}^3) ions are nondegenerate, Fig. 1.2) and develop the orbital ordering shown in Fig. 1.3. Both the charge ordering (CO) and the OO occur simultaneously at the same temperature, although from some data it follows that probably the CO is the driving force, and the OO follows it [10]; this however is still an open question.

According to the well-known Goodenough–Kanamori–Anderson rules (see e.g. [1, 6, 7]) the magnitude and even the sign of the magnetic exchange depend on the type of orbitals that are occupied. Thus if the orbitals occupied by one electron (half-filled orbitals) are directed towards each another, one has a strong antiferromagnetic coupling; if however these orbitals are directed away from each other (are mutually orthogonal) we would have a ferromagnetic interaction. That is why the undoped $LaMnO_3$ (Fig. 1.2) has the A-type magnetic ordering –the spins in the (x, y)-plane order ferromagnetically, the next xy-layer being antiparallel to the first one.

There are two more regions of the phase diagram of Fig. 1.1 in which orbital effects apparently play an important role, although the detailed picture is less clear. These are the low-doped region $0.1 \leq x \leq 0.2 - 0.3$ (depending on the specific system considered) in which one often observes the ferromagnetic insulating (FI) and presumably charge-ordered phase. This is the case of $La_{1-x}Ca_xMnO_3$ $(0.1 \leq x \leq 0.25)$, $La_{1-x}Sr_xMnO_3$ close to $x = \frac{1}{8}$ $(0.1 \leq x \leq 0.18)$ [11, 12] and $Pr_{1-x}Ca_xMnO_3$ $(0.15 \leq x \leq 0.3)$ [9].

It is rather uncommon to have a FI state: typically insulating materials of this class are antiferromagnetic, and ferromagnetism goes hand in hand with metallicity, which is naturally explained in the model of double exchange [13]. The only possibility to obtain the FI state in perovkites is due to a certain particular orbital ordering favourable for ferromagnetism [6] (the FI state can appear also in systems in which there exists the 90°-superexchange: the TM–O–TM angle is close to 90°). But what is the detailed ordering in this low-doped region, is not completely clear, see Section 2.1.

Another interesting, and much less explored, region is the overdoped manganites, $x > 0.5$. Typically in this case we have an insulating state, sometimes with the CO and OO state in the form of stripes [14] or bistripes [15]. The choice between these two options is still a matter of controversy (see e.g. [14, 16]), as well as the detailed type of magnetic ordering in this case. We will return to this point in section 4.2. When discussing the properties of overdoped manganites at $x > 0.5$, one should mention an important fact: the very strong asymmetry of the typical phase diagram of manganites. As seen e.g. from Fig. 1.1, there usually exists a rather large ferromagnetic metallic region (FM) for $x < 0.5$, but almost never for $x > 0.5$ (only rarely one observes bad metallic behavior and unsaturated ferromagnetism in a narrow concentration range in some overdoped manganites [17]). However from the standard double-exchange model one can expect the appearance of a FM phase not only in hole-doped $LaMnO_3$ $(x < 0.5)$ but in electron-doped

$CaMnO_3$ ($x > 0.5$) as well. Orbital degeneracy may play some role in explaining this asymmetry [18] –see section 4.

There exists also a problem as to what are the orbitals doing in the optimally doped ferromagnetic and metallic manganites. Usually one completely ignores orbital degrees of freedom in this regime, at least at low temperatures; this is supported by the experimental observations that the MnO_6-octahedra are completely regular in this case. But orbital degrees of freedom cannot just vanish. In this doping regime there is a strong competition between the tendency of orbitals to order locally and the kinetic energy of the charge carriers that tends to destroy long range orbital order. This is comparable to the situation in High T_c superconductors, where the long-range antiferromagnetic order of, in this case, spins is frustrated by mobile charge carriers. In an analogous way the mobile holes in optimally doped manganites can melt the orbital order: in the ferromagnetic metallic phase of the manganites the orbital degrees of freedom do not simply disappear, but instead the orbitals are "rotating" very fast and may form resonating orbital bonds, see Section 3. Another option –orbital ordering of a new type with "complex orbitals" is discussed in Section 2.2.

1.2. Mechanisms for Orbital Ordering

Before discussing particular situations in different doping ranges, it is worthwhile to address briefly the general question of possible interactions of degenerate orbitals which can lead to orbital ordering. In transition metal compounds there are essentially two such mechanisms. The first one is connected with the Jahn-Teller interaction of degenerate orbitals with the lattice distortions, see e.g. [19]. Another mechanism was proposed in 1972 [20], see also [2], and is a direct generalization of the usual superexchange [21] to the case of orbital degeneracy.

A convenient mathematical way to describe orbital ordering is to introduce operators T_i of the pseudospin $\frac{1}{2}$, describing the orbital occupation, so that e.g. the state $|T^z = \frac{1}{2}\rangle$ corresponds to the occupied orbital $|3z^2 - r^2\rangle$, and $|T^z = -\frac{1}{2}\rangle$ to $|x^2 - y^2\rangle$. The first one corresponds to a local elongation of the O_6-octahedra (distortion coordinate $Q_3 > 0$), see Fig. 1.4, and the second –to local contraction $Q_3 < 0$ [22]. The second degenerate E_g-phonon which can also lift electronic e_g-degeneracy, Q_2, see Fig. 1.4, corresponds to a pseudospin operator T^x. One can describe an arbitrary distortion and corresponding wave function by linear superpositions of the states $|T^z = +\frac{1}{2}\rangle$ and $|T^z = -\frac{1}{2}\rangle$:

$$|\theta\rangle = \cos\tfrac{\theta}{2}|\tfrac{1}{2}\rangle + \sin\tfrac{\theta}{2}|-\tfrac{1}{2}\rangle \tag{1.1}$$

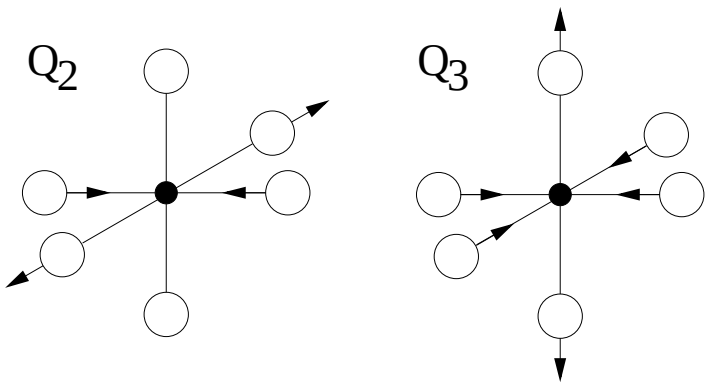

Figure 1.4. Schematic representation of the Q_2 and Q_3 Jahn-Teller distortions of a MnO_6 octahedron.

where θ is an angle in (T^z, T^x)-plane.

The Jahn-Teller mechanism for orbital ordering starts from the electron–phonon interaction, which in our case can be written in the form

$$H = \sum_{iq} g_{iq}[T_i^z(b_{3q}^\dagger + b_{3,-q}) + T_i^x(b_{2q}^\dagger + b_{2,-q})] + \sum_{\alpha q} \omega_{\alpha q} b_{\alpha q}^\dagger b_{\alpha q} \qquad (1.2)$$

where $\alpha = 2; 3$ and $b_3^\dagger$ and $b_2^\dagger$ are the phonon operators corresponding to Q_3 and Q_2 local modes. Excluding the phonons by a standard procedure, one obtains the orbital interaction having the form of a pseudospin–pseudospin interaction

$$H_{eff} = \sum_{ij} J_{ij}^{\mu\nu} T_i^\mu T_j^\nu \qquad (1.3)$$

where

$$J_{ij} \sim \sum_q \frac{g_q^2}{\omega_q} e^{iq(R_i - R_j)} \qquad (1.4)$$

and $\mu, \nu = x, z$. Due to different dispersion of the different relevant phonon modes, and due to the anisotropic nature of electron–phonon coupling, the interaction (1.3) is in general anisotropic.

Similarly, the exchange mechanism of orbital ordering may be described by the Hamiltonian containing the pseudospins T_i, but it contains also the ordinary spins $\vec{S}_i$. The effective superexchange Hamiltonian can be derived starting from the degenerate Hubbard model [20], and it has schematically the form

$$H = \sum_{ij} \{J_1 \vec{S}_i \vec{S}_j + J_2(T_i T_j) + J_3(\vec{S}_i \vec{S}_j)(T_i T_j)\}. \qquad (1.5)$$

Here the orbital part (T_iT_j), similar to (1.3), is in general anisotropic, whereas the spin exchange is Heisenberg-like. In contrast to the Jahn-Teller induced interaction, the exchange mechanism describes not only the orbital and spin orderings separately, but also the coupling between them (last term in (1.5)). This mechanism is rather successful in explaining the spin and orbital structure in a number of materials [2, 20], including $LaMnO_3$ (for the latter system one has to invoke also the anharmonicity effects [20] –see also [23]).

As to the electron-lattice interaction, typically one includes mostly the coupling with the local –i.e. optical– vibrations [24]. However no less important may be the interaction with the long-wavelength acoustical phonons, or, simply speaking, with the elastic deformations. Generally, when one puts an impurity in a crystal, e.g. replacing the small Mn^{4+} ion in $CaMnO_3$ by the somewhat larger Mn^{3+} ion, which in addition causes a local lattice distortion due to the Jahn-Teller effect (i.e. we replace a "spherical" Mn^{4+} ion by an "ellipsoidal" Mn^{3+}), this creates a strain field which is in general anisotropic and decays rather slowly, as $1/R^3$ [25, 26]. A second "impurity" of this kind "feels" this strain, which leads to an effective long-range interaction between them. This can naturally lead to the spontaneous formation of different superstructures in doped materials [27, 28]. Thus, there may appear vertical or diagonal stripes, even for non-Jahn-Teller systems. In case of manganites one can show that there appears e.g. an effective attraction between $3x^2-r^2$ and $3y^2-r^2$-orbitals in x and y-direction; this immediately gives the orbital ordering of $LaMnO_3$-type shown in Fig. 1.2. For $x = 0.5$, assuming the checkerboard charge ordering, one gets from this mechanism the correct orbital ordering shown in Fig. 1.3 [27, 28]. And for overdoped manganites one can get either single or paired stripes, depending on the ratio of corresponding constants: One can show [24, 27, 28] that for a diagonal pair like the ones in Fig. 1.14, one gets an attraction of the same orbitals $3x^2 - r^2$ and $3x^2 - r^2$ or $3y^2 - r^2$ and $3y^2 - r^2$, but repulsion of $3x^2 - r^2$ and $3y^2 - r^2$. Thus, if one takes into account only these nearest neighbour diagonal interactions, the single stripe phase of Fig. 1.14 would be more favourable than the paired stripes of the Fig. 1.14. However the latter may in principle be stabilizes by more distant interactions like those for a pair of Mn^{3+} ions along x and y-directions in Fig. 1.14. Which state is finally more favourable, is still not clear, see Ref. [28].

2. Orbital order for $x < 1/2$

In the previous section we have given some examples that show that the interaction of orbital degrees of freedom among themselves and the interaction with electron spins or with the lattice, can give rise to long-range orbital ordered states. Experimentally the manganites seem to be especially susceptible to an orbital order instability at commensurate doping concentrations: the undoped system is a canonical example of an orbitally-ordered Mott insulator and for $x = 1/2$ orbitals are ordered in most manganites. Below we discuss the situation for $x = 1/8$ and $x = 1/4$ and the possibility of orbital order in the metallic phase.

Every ordered state has one or more elementary excitations related to the actual symmetry that is broken by the long-range order. In spin systems this symmetry is often continuous, which leads to the occurence of a Goldstone mode, in this case a spin-wave –magnon– that has a vanishing excitation energy when its wavelength is very long. Related to the ordering of orbitals there should therefore be an elementary excitation with orbital character: the orbiton. Recently this orbital wave was actually observed experimentally [47]. In this and the next section we discuss some of its properties, emphasizing that the orbital mode is gapped and that it strongly interacts with lattice and spin degrees of freedom [46].

2.1. Undoped and lightly doped manganites

As already mentioned in section 1, typically there exist a ferromagnetic insulating region at low doping ($0.1 \lesssim x \lesssim 0.18$ for the LaSr system, $x \lesssim 0.25$ for LaCa, $0.15 \lesssim x \lesssim 0.3$ for PrCa). The problem is to explain the origin of the FI state in this case. Apparently it should be connected with an orbital ordering of some kind; but what is the specific type of this ordering, is largely unknown.

The most complete, but still controversial, data exist on the LaSr-system close to $x = 1/8$. There exists a superstructure in this system [29, 11], and an orbital ordering was detected in the FI phase in [12]. Certain orbital superstructures were also seen by the resonant X-ray scattering in $Pr_{0.75}Ca_{0.25}MnO_3$ [33]. Both these systems, however, were looked at by this method only at one k-point [300], which is not sufficient to uniquely determine the type of orbital ordering. The existing structural data, or rather the interpretation of this data, is still controversial [30, 31, 32].

Theoretically two possibilities were discussed in the literature [34, 35]. First of all one can argue that when one puts a Mn^{4+} ion into Mn^{3+} matrix, the orbitals of all the ions surrounding the localized hole (Mn^{4+}) would be directed towards it, see Fig. 1.5*a* [35, 36]. One can call such

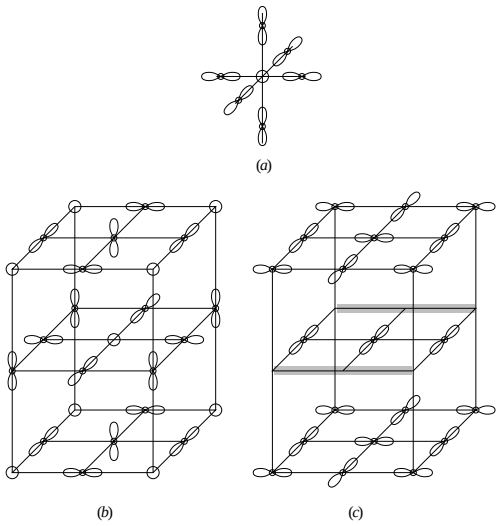

Figure 1.5. Orbital polarons and possible types of orbital ordering in low doped manganites: (*a*) Orbital polaron close to a Mn^{4+} ion; (*b*) Ordering of orbital polarons for $x = 0.25$ in a bcc-lattice; (*c*) An alternative charge and orbital ordering, obtained for $x = 1/8$ in [34]. Notations are the same as in Figs. 1.3 and 1.14. Shaded lines– "stripes" containing holes.

state an orbital polaron. We use the concept of 'orbital polaron' in a rather loose sense here and for a somewhat more formal discussion we refer to Section 3.3. These polarons, which according to Goodenough–Kanamori–Anderson rules would be ferromagnetic, can then order e.g. as shown in Fig. 1.5*b* for $x = 0.25$. The calculations carried out in [35] show that this state is indeed stable, and it corresponds to a ferromagnetic insulator. Thus it is a possible candidate for a FI state at $x \simeq 1/4$ e.g. in Pr–Ca system.

However there exist an alternative possibility. Calculations show [34] that a similar state with ordered polarons is also locally stable for $x \simeq 1/8$. But it turned out that the lower energy is reached in this case by different type of charge and orbital ordering, Fig. 1.5*c* [34]: the holes are localized only in every second xy-plane, so that one such plane containing only Mn^{3+} ions develops the orbital ordering of the type of $LaMnO_3$, Fig. 1.2, and the holes in the next plane concentrate in "stripes", e.g. along x-direction. This state also turns out to be ferromagnetic, and the superstructure obtained agrees with the experimental results of [29] and [11] for $La_{1-x}Sr_xMnO_3$, $x \simeq 1/8$. One can think that the situation can be also similar for $x \simeq 1/4$ which would agree with the data of [33]. This type of the charge ordering (segregation of holes in every second plane)

may be favourable due to an extra stability of the $LaMnO_3$-type orbital ordering, strongly favoured by the elastic interactions [28], as discussed in section 1. A "mixed" possibility is in principle also possible: there may exist for example a similar charge segregation into a hole-rich and hole-poor plane, but the orbitals may rather behave as is shown in Fig. 1.5*a*, i.e. contrary to fig 1.5*c*, there may be partial occupation of $3z^2-r^2$-orbitals at certain sites.

2.2. Possible orbital ordering in metallic phase

Let us discuss the most important phase –that of optimal doping, $x \simeq 0.3$ - 0.5. In most cases the systems in this doping range are ferromagnetic and metallic at low temperatures, although the residual resistivity is usually relatively large.

Now, the question is: what are the orbitals doing in this phase? Experimentally one observes that the macroscopic Jahn-Teller ordering and corresponding lattice distortion is gone in this regime. La–Ca system remains orthorhombic in this concentration range, but that is due to the tilting of the O_6 octahedra, the octahedra themselves being regular (all the Mn–O distances are the same). The structure of the La–Sr manganites in this regime is rhombohedral, but again all the Mn–O distances are equal. Moreover even the local probes such as EXAFS or PDF (pair distribution function analysis of neutron scattering) [37], which detect local distortions above and close to T_c, show that for $T \to 0$ they completely disappear, and MnO_6-octahedra are regular even locally.

What happens then with the orbital degrees of freedom? There are several possibilities. One is that in this phase the system may already be an ordinary metal, the electronic structure of which is reasonably well described by the conventional band theory. In this case we should not worry about orbitals at all: we may have a band structure consisting of several bands, some of which, not necessarily one, may cross Fermi-level, and we should not speak of orbital ordering in this case, just as we do not use this terminology and do not worry about orbital ordering in metals like Al or Nb which often have several bands at the Fermi-level.

If however there exist strong electron correlations in our system (i.e. the Hubbard's on-site repulsion U is bigger that the corresponding bandwidth) –one should worry about it. The orbital degrees of freedom should then do something. In principle there exists two options. One is that the ground state would still be disordered due to quantum fluctuations, forming an orbital liquid [38], similar in spirit to the RVB state of the spin system (we can speak of the pseudospin RVB state). We discuss this physics in the next section.

There is also an alternative possibility: there may in principle occur an orbital ordering of a novel type, without any lattice distortion, involving not the orbitals of the type (1.1), but the *complex* orbitals – linear superpositions of the basic orbitals $3z^2 - r^2$ and $(x^2 - y^2)$ with the complex coefficients, e.g.

$$|\pm\rangle = \frac{1}{\sqrt{2}}\Big(|3z^2 - r^2\rangle \pm i|x^2 - y^2\rangle\Big). \tag{1.6}$$

This possibility was first suggested in [39] and then explored in [40, 41]; independently a similar conclusion was reached a bit later in [42]. One may easily see that the distribution of the electron density in this state is the same in all three directions, x, y and z. Thus this ordering does not induce any lattice distortion –the MnO_6 octahedra remain regular, and the system is cubic (if we ignore tilting of the octahedra). On the other hand, the state with complex coefficients, as always is the case with complex wave functions, breaks time-reversal invariance, i.e. this state is in some sense magnetic. One can show however that the magnetic dipole moment in this case is zero –it is well known that the orbital moment is quenched in e_g-states (these states are actually $|l^z = 0\rangle$ and $\frac{1}{\sqrt{2}}(|2\rangle + |-2\rangle)$ states of the $l = 2$ d-orbitals). Similarly, the magnetic quadrupole moment is also zero, by parity arguments. The first nonzero moment in this state is a magnetic octupole. Indeed, the actual order parameter in this case is the average $\eta = \langle M_{xyz}\rangle = \langle \mathrm{S} L_x L_y L_z\rangle \neq 0$ where l_α are the components of the orbital moment $l = 2$ of d-electrons, and S means the symmetrization. This operator is actually proportional to the T^y-operator of pseudospin, i.e. the order parameter of this type of orbital ordering is $\eta = \langle T^y\rangle$. One can visualize this state as the one in which there exist orbital currents at each unit cell.

2.3. Orbitons: orbital excitations

Each time we have certain ordering in solids, corresponding excitations should appear. The quadrupolar charge ordering –orbital ordering– should give rise to elementary excitations with orbital signature, as this order causes a breaking of symmetry in the orbital sector. These excitations –we may call them orbitons– were first discussed shortly in [2, 20] and recently were studied theoretically in several papers, e.g. in [43, 44, 45, 46]. One of the problems that could complicate an experimental observation of these excitations, is the usually rather strong Jahn-Teller coupling of orbital degrees of freedom with the lattice distortions. This could make it very difficult, if not impossible, to "decouple" orbitons from phonons. And indeed the experimental efforts to observe orbitons were unsuccessful for many years. A breakthrough came only

recently when the group of Y. Tokura managed to observe the manifestations of orbital excitations in Raman scattering on untwinned single crystals of $LaMnO_3$ [47].

The observed orbitons were interpreted by the authors as being due to electron correlations [47], but in the comment that accompagnied this publication it was immediately mentioned that here the coupling to phonons can also be very important [48]. Let us briefly discuss the question of the origin of orbitons; this is also important as they, in turn, have a large effect on spin [45, 49] and charge excitations [50, 51, 52], as we discussed in the previous section.

The physical aspects of the coupling between the orbital excitation and Jahn-Teller phonons can be illustrated by considering the orbital and phonon excitations as dispersionless. We can view this as a reasonable first approximation because orbital excitations are always gapped (see next section) and Jahn-Teller lattice excitations are optical phonons. Applying this simplification to Eqs.(1.2) and (1.3) leads to the single-site Hamiltonian [46]

$$\begin{aligned} H_{loc} &= [\bar{J} + 2g(b_3^\dagger + b_3)]q^\dagger q + \omega_0(b_3^\dagger b_3 + b_2^\dagger b_2) \\ &+ g(q^\dagger + q)(b_2^\dagger + b_2), \end{aligned} \tag{1.7}$$

where the q operator describes an orbiton excitation, $b_{2,3}$ are the $Q_{2,3}$ phonon modes and $\bar{J} = 3J + 4g^2/\omega_0$, where g is the electron-phonon coupling constant, ω_0 the JT phonon frequency and J the superexchange energy. Let us discuss three important consequences of the orbiton-phonon coupling in Eq. (1.7). First, the coupling to the lattice moves the orbiton to higher energy an amount $4g^2/\omega_0$. This shift has a straightforward physical meaning: it is the phonon contribution to the crystal-field splitting of the e_g-states caused by the static Jahn-Teller lattice deformation. The effective orbital excitation energy is the sum of the local orbital exchange energy and static phonon contribution to the crystal-field splitting.

If, however, an orbital excitation is made, it strongly interacts with the Q_3 phonon, so that the orbital excitation can be dynamically screened by the Jahn-Teller phonons and lowered in energy. The crystal-field splitting and screening are strongly competing as both are governed by the energy scale set by the electron-phonon coupling. Finally, the orbital and Q_2 phonon modes mix, as is clear from the last term of H_{loc}. This implies that the true eigenmodes of the coupled orbital-phonon system have both orbital and phonon character.

In general, the mixing of orbital and phonon mode gives rise to extra phonon satellites in the orbiton spectral function at energy intervals of ω_0. Vice versa, due to this mixing, a low intensity orbital satellites

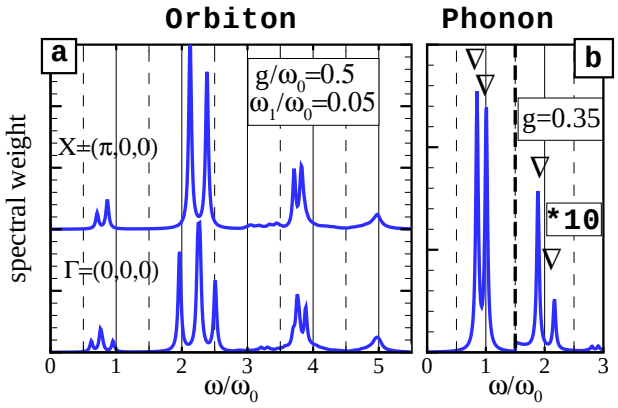

Figure 1.6. (a) Orbiton spectral function at the Γ and X-point, $g = \omega_0/2$. (b) Spectrum of the Raman-active A_g and B_{1g} phonon modes for $g/\omega_0 = 0.35$. The experimental peak positions are indicated by ∇. For $\omega > \omega_0$ the spectral weight is multiplied by 10, see Ref. [46].

at $\approx 3J$ will be present in the Q_2 phonon spectral function. As discussed above, the most plausible estimates of the Jahn-Teller energy ($E_{JT} = 4g^2/\omega_0$) are $E_{JT} \approx 200 - 300$ meV, and the superexchange $J \approx 40$ meV. With these estimates, keeping in mind the results described above –the strong mixing of the orbital excitation and the phonons– one comes to the conclusion that the features at 150 meV observed in the Raman experiment [47], interpreted there as pure orbital excitations, are rather the orbiton-derived satellites in the phonon spectral function, see Fig. 1.6 [46]. A framework beyond the toy model described above is needed to establish the relevance of such an interpretation, and to establish the exact nature of the satellites in the Raman spectra: this is still an open issue, both experimentally and theoretically. But it is clear that the elementary excitations of an orbital ordered system are mixed modes with both orbital and phonon character, or, in other words, are determined by both electron correlation effects and the electron-lattice interaction.

3. Quantum effects; optimal doping

Below the cooperative orbital/Jahn-Teller transition temperature, a long-range coherence of orbital polarization sets in, and spin-exchange interactions on every bond are fixed by the Goodenough-Kanamori rules [1, 6, 7, 53]. Implicit in this picture is that the orbital splittings are large enough so that we can consider orbital populations as classical numbers. Such a classical treatment of orbitals is certainly justified when orbital order is driven by strong cooperative lattice distortions that lead to a

large splitting of the –initially degenerate– orbital levels. In this limit the orbital excitations are more or less localized high-energy quadrupole moment (or crystal-field) transitions, and therefore they effectively just renormalize spin degrees of freedom but otherwise do not effect much the physical properties of the system at low energy scales.

Quantum effects, however, can start to dominate the ground state properties and elementary excitations when classical order is frustrated by some interaction that opposes the tendency of the orbitals to order. The reason that this might very well be the case in some regions of the phase diagram of the manganites is that orbitals strongly interact with spins via the superexchange and that orbital order is frustrated by the kinetic energy of carriers in a metallic system. But the actual situation in manganites is still under debate; while in the undoped case the orbital excitations are rather high in energy and therefore quite decoupled from the spins, there are many indications that orbital dynamics play an essential role in the physics of doped manganites.

In this Section we discuss several physical examples and some theoretical models that show that there is a strong dynamical interplay between orbital fluctuations and spin and charge degrees of freedom. Both spin exchange and charge motion are highly sensitive to the orbital bonds, and the basic idea is that the interaction energy cannot be optimized simultaneously in all the bonds: this leads to the peculiar frustrations and quantum resonances among orbital bonds. Of course a classical treatment in such cases gives very poor estimates of energies, and the quantum dynamics of the coupled orbital-spin-charge system becomes of crucial importance, as we illustrate below in the context of several theoretical models with coupled orbital, spin and charge degrees of freedom. Thus the important physics, quantum effects, largely depend on some particular properties of orbital systems, notably the frustration in the orbital sector, which are absent in canonical spin and spin-charge models, e.g. the t-J model. To explain this, we devote some time to a more theoretical discussion, treating some orbital and spin-orbital models (Section 3.1 and 3.2); later on in this chapter we will apply these concepts to the discussion of properties of manganites in the cubic metallic phase (Sections 3.4 and 3.5)

3.1. Superexchange and spin-orbital models

Quantum fluctuations of the orbitals originate mainly from two kind of interactions. First we discuss the superexchange interaction, and the second mechanism –the very effective frustration of orbitals by doped holes– we describe later on.

Let us take as an example a toy version of the full superexchange model (proposed by Kugel and Khomskii [2]). On a three-dimensional cubic lattice it takes the form:

$$\begin{aligned} H &= \sum_{\langle i,j \rangle} \hat{J}_{ij}^{(\gamma)} (\vec{S}_i \vec{S}_j + \frac{1}{4}), \\ \hat{J}_{ij}^{(\gamma)} &= J(T_i^{(\gamma)} T_j^{(\gamma)} - \frac{1}{2} T_i^{(\gamma)} - \frac{1}{2} T_j^{(\gamma)} + \frac{1}{4}), \end{aligned} \tag{1.8}$$

with $J = 4t^2/U$, where t and U are, respectively, the hopping integral and on-site Coulomb repulsion in the Hubbard model for two-fold degenerate e_g-electrons at half filling. The structure of $T_i^{(\gamma)}$ depends on the index γ which specifies the orientation of the bond $\langle ij \rangle$ relative to the cubic axes a, b and c:

$$T_i^{(a/b)} = \frac{1}{4}(-\sigma_i^z \pm \sqrt{3}\sigma_i^x), \qquad T_i^{(c)} = \frac{1}{2}\sigma_i^z, \tag{1.9}$$

where σ^z and σ^x are the Pauli matrices. Physically the T operators describe the dependence of the spin-exchange interaction on the orbitals that are occupied, and the main feature of this model –as is suggested by the very form of Hamiltonian (1.8)– is the strong interplay between spin and orbital degrees of freedom. It was recognized first in Ref. [49] that this simple model contains rather nontrivial physics: the classical Néel state in Eq. (1.8) (where $\langle \vec{S}_i \vec{S}_j \rangle = -1/4$) is infinitely degenerate in the orbital sector; this extra degeneracy must be lifted by some mechanism. Before discussing this mechanism, let us first elaborate on this degeneracy and the importance of quantum effects in this case. We first notice that the effective spin exchange constant in this model is definite positive ($\langle J_{ij}^{(\gamma)} \rangle \geq 0$) for any configuration of orbitals, where its value can vary from zero to J, depending on the orientation of orbital pseudospins. We therefore expect a simple two-sublattice antiferromagnetic, G-type, spin order. There is however a problem: a classical G-type ordering has cubic symmetry and can therefore not lift the orbital degeneracy, not even locally. In more formal terms, the spin part $(\vec{S}_i \vec{S}_j + 1/4)$ of the Hamiltonian (1.8), in mean field approximation, simply becomes zero in this state for all bonds, so that these orbitals effectively do not interact –they are completely uncorrelated– and hence retain full rotational freedom on every lattice site. In other words, we gain no energy from the orbital interactions that are present in the model. This shows that from the point of view of the orbitals the classical Néel state is energetically a very poor state of the system.

The mechanism for developing intersite orbital correlations (and hence to gain energy from orbital ordering) must involve a strong deviation in

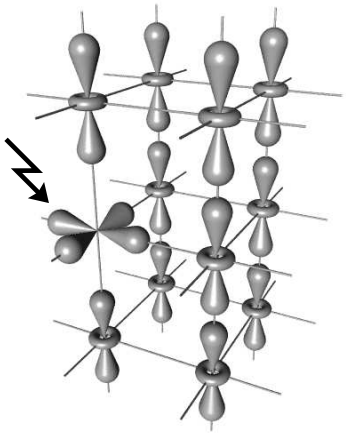

Figure 1.7. $|3z^2 - r^2\rangle$-orbital order which leads to weakly coupled AF spin chains ($J_c = J$, $J_\perp = J/16$). As discussed in Refs. [45, 58], this type of orbital ordering provides the largest energy gain due to quantum spin fluctuations. An orbital flip (indicated by an arrow) modulates the strength of the neighboring exchange bonds, breaking the c chain. In the classical Néel state, such orbital excitations cost no energy [49, 57]. Due to the presence of strong quasi one-dimensional spin fluctuations, however, a finite orbital gap opens through the order from disorder mechanism, thus stabilizing this structure.

the spin configuration from the Néel state –a deviation from $\langle \vec{S}_i \vec{S}_j \rangle = -\frac{1}{4}$. This implies an intrinsic tendency of the system to develop low-dimensional spin fluctuations which can most effectively be realized by an ordering of orbitals as shown in Fig. 1.7. In this situation the effective spin interaction is quasi-one-dimensional along the chains in the c-direction so that quantum spin fluctuations are enhanced as much as possible and quantum energy is gained from the bonds along the chain. Here $\langle \vec{S}_i \vec{S}_j + \frac{1}{4} \rangle < 0$, so that the effective orbital (pseudospin) exchange is indeed ferromagnetic, which leads to the orbital structure shown in Fig. 1.7. At the same time the cubic symmetry is explicitely broken, as fluctuations of spin bonds are different in different directions. This leads to a finite splitting of e_g-levels, and therefore an orbital gap is generated. One can say that in order to stabilize the ground state, orbital order and spin fluctuations support and enhance each other –a situation that is very similar to Villain's order from disorder phenomena known previously from frustrated spin systems [54, 55, 56].

From the technical point of view, it is obvious that a conventional expansion about the classical Néel state would fail to remove the orbital degeneracy: only quantum fluctuations can lead to orbital correlations.

This is precisely the reason why in a linear spin-wave approximation one does not obtain an orbital gap, and low-energy singularities appear [49, 57]. The problem was resolved in Refs.[45, 58]: the singularities vanish once quantum spin fluctuations are explicitely taken into account in the calculations of the orbiton spectrum. These fluctuations generate a finite gap for single orbital as well as for any composite spin-orbital excitation, and in this way the spin fluctuations remove the orbital frustration problem. The long-range spin-orbital order indicated in Fig. 1.7 is stable against residual interactions because of the orbital gap (of the order of $J/4$), and because of the small, but finite, coupling between spin chains.

In general the Kugel-Khomskii model is a very nice example of how an apparently three-dimensional system may by itself develop low-dimensional quantum fluctuations. We find it quite interesting and amusing that these quantum fluctuations do not only coexist with a weak three-dimensional staggered spin moment, but that they are actually of vital importance to stabilize this long-range order by generating an orbital gap and intersite orbital correlations. The physical origin of this peculiar situation is, of course, the strong spatial anisotropy of the e_g-orbital wave functions. Because of this anisotropy it is impossible to optimize all the bonds between Mn^{3+} ions simultaneously; this results in orbital frustration. The best the system can finally do, is to make specific strong and weak bonds in the lattice, whereby it reduces the effective dimensionality of the spin system in order to gain quantum energy. At the same time tunneling between different orbital configurations is suppressed: the spin fluctuations produce an energy gap for the rotation of orbitals.

3.2. Orbital-only models

Let us consider for the moment the spins to be frozen in a ferromagnetic configuration, and ask how the orbitals would behave in this case. The model (1.8) then reads

$$H_{orb} = A \sum_{\langle ij \rangle_\gamma} T_i^{(\gamma)} T_j^{(\gamma)}, \tag{1.10}$$

where $T_i^{(\gamma)}$ is given by Eq. (1.9) and $A = J/2$. This limit has actually been considered in Ref.[59] as a model system to describe orbital dynamics in an undoped orbitally degenerate ferromagnet and for the ferromagnetic insulating phase of underdoped manganites. In the latter case this mapping is not quite satisfying because the ferromagnetic insulator is in fact stabilized by frozen-in doped holes that strongly af-

fect the orbitals in their neighborhood, as was discussed in Section 2.1. The model (1.10) is clearly anisotropic and in that respect underlines the important difference between orbital excitations and conventional spin dynamics. Another very closely related model is a so-called "cubic" model defined as follows:

$$H_{cub} = \frac{A}{4}(\sum_{\langle ij\rangle_a} T_i^x T_j^x + \sum_{\langle ij\rangle_b} T_i^y T_j^y + \sum_{\langle ij\rangle_c} T_i^z T_j^z), \qquad (1.11)$$

where along each a,b and c crystallographic axis only one of the respective orbital operators T^x, T^y and T^z is active. In this "cubic" model the bond anisotropy in Hamiltonian 1.10 is taken to the extreme. Although the model is not directly applicable to the manganites, it is simpler than the model in Eq. (1.10), but it still contains the essential bond anisotropy and degeneracy that makes orbital models so different from spin Hamiltonians. This model has been proposed and discussed in the context of orbital frustrations already in the 1970's [60]. It is interesting to notice that precisely this "cubic" model appears in cubic titanates as a magnetic anisotropy Hamiltonian [61].

We discuss the two models in Eq (1.10),(1.11) in parallel as they display very similar peculiarities in the low-energy limit. As pseudospins in both models interact antiferromagnetically along all bonds, a staggered orbital ordered state is expected to be the ground state of the system. In the three-dimensional system at the orbital degeneracy point, however, linear spin-wave theory leads to a gapless two-dimensional excitation spectrum. This results in an apparent instability of the ordered state at any finite temperature [59], an outcome that sounds at least counter-intuitive. Actually, the problem is even more severe: a close inspection shows that the interaction corrections to the orbiton excitations diverge even at zero temperature, manifesting that the linear spin-wave expansion about a classical staggered orbital, Néel-like, state is not adequate in this case.

The origin of these problems was recently clarified in Refs.[61, 62]. By symmetry, there are only a finite number of directions (three equivalent cubic axes), one of which will be selected by a staggered pseudospin order parameter. Since this breaks only discrete symmetry, the excitations about the ordered state must have a gap. A linear spin wave theory fails however to give the gap, because Eqs.(1.10),(1.11) acquire a rotational symmetry in the limit of classical spins. This results in an infinite degeneracy of classical states, and an accidental pseudo Goldstone mode appears, which is however not a symmetry property of the original quantum models (1.10),(1.11). This artificial gapless mode leads to low-energy divergencies that arise because the coupling constant for the

interaction between orbitons does not vanish at zero momentum limit, as it would happen for a true Goldstone mode. Hence the interaction effects are non-perturbative.

At this point the order from disorder mechanism comes again into play: a particular classical state is selected so that the fluctuations about this state maximize the quantum energy gain, and a finite gap in the excitation spectra opens, because in the ground state of the system the rotational invariance is broken. An orbital gap $\Delta \simeq A/2$ in the model (1.10) has been estimated in Ref. [62, 63], which has to be compared with the full orbiton dispersion of $3A$. Similarly, the "cubic" model with nearest-neighbor interactions shows long-range orbital order and has an excitation gap $\Delta \simeq A$ [61]. It should be noticed however, that while ground state and gap issue in models (1.10),(1.11) are more or less settled, further studies are required to fully characterize the excitation spectra. Of particular interest are damping effects, as we expect substantial incoherent features in the orbiton modes because of the strong interaction between low-energy ($\sim \Delta$) orbitons.

What can we learn from the examples above? The calculation of the excitation spectrum in systems with orbital degeneracy is somewhat involved even in the half filled, insulating limit. This is due to the peculiar frustration of superexchange interactions, which leads to infrared divergencies when linear spin wave theory is applied [49, 57, 59]. That such divergencies occur in lowest order approximations is a universal feature of e_g-orbital models on cubic lattice –it reflects the special symmetry properties of e_g-orbital pseudospins. To calculate the excitation spectrum a more careful treatment of quantum effects is then required.

The main message is that orbital ordering, unlike spin ordering, is not accompanied by a simple Goldstone mode. Rather, collective orbiton excitations always have a finite gap and we also expect a substantial incoherent damping over all momentum space. This distinct feature of the orbitons has to be kept in mind for the interpretation of experimental data. Of course the precise way of how an orbiton gap is generated, depends on the model, but an order from disorder scenario seems to be a rather common mechanism to resolve the frustration of classically degenerate orbital configurations. It is interesting to note that if one takes instead a similar model but with long-range interaction, e.g. the classical model with dipole-dipole interaction, the conclusion about the long-range order might be modified; it was shown in [64] that there is no long-range order of the type shown in Fig. 1.2 in the dipole model in two- and three-dimensional systems.

Although this review focuses on e_g-orbital dynamics, it is worthwhile to mention at this point that orbital frustration is in fact a very general

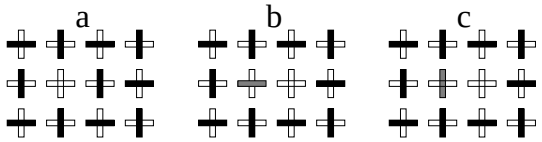

Figure 1.8. Schematic representation of a hole in an orbital ordered ground state (a). The occupied (empty) orbitals are shown as filled (empty) rectangles. The hole can move either without disturbing the orbital order (b), or by creating orbital excitations (c).

property of all orbital degenerate cubic perovskite compounds, including those with three-fold t_{2g} orbital degeneracy. In this case the situation is actually even more dramatic because the degeneracy of t_{2g} level is larger [65], which enhances quantum effects [66]. In addition to the frustration that is present in the e_g-system, there also exists the possibility to form quantum singlets and resonating valence bonds among t_{2g} orbitals (see for the details Refs. [61, 67]). Therefore quantum tunneling between different local orbital configurations may occur. The cubic titanate $LaTiO_3$ is an outstanding example: it was recently observed [68] that orbitals in this Mott insulator remain disordered even at low temperature, which can be explained by the formation of a coherent quantum liquid state [67]. The cubic vanadates are also interesting in this respect, although they are different because of the larger spin value. In this case the spin-orbital frustration is again resolved by the order from disorder mechanism with the help of low-dimensional orbital fluctuations [69].

3.3. Orbital-charge coupling, orbital polarons

We turn now to doping effects in manganites and first discuss the low doping regime. A doped hole in the Mott insulator strongly interacts with a variety of low-energy degrees of freedom, which leads to polaronic effects. In a pure spin-charge $t-J$ model, as are used for the cuprates, a hole breaks the spin bonds, and more importantly, frustrates spin order when it hops around. In manganites, the presence of orbital degeneracy brings about new degrees of freedom that control the dynamics of holes. As is discussed in detail in Ref.[51, 52], there are in general two channels of orbital-charge coupling. The first one, that acts via the electron-transfer term of the orbital $t-J$ Hamiltonian [70], is very similar to the spin-charge coupling mentioned above. This interaction of holes with orbital degrees of freedom changes the character of the hole motion: the scattering on orbital excitations leads to a suppression of the coherent

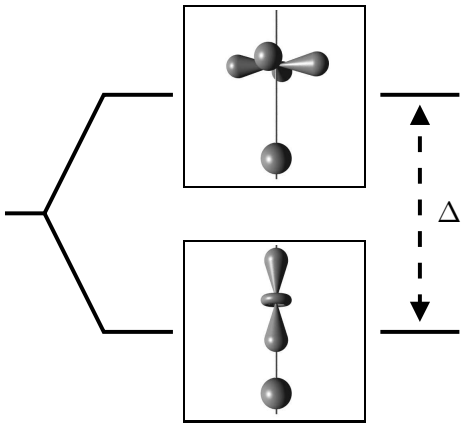

Figure 1.9. Polarization of e_g-levels on sites next to a hole [51]: Bond stretching phonons and Coulomb interaction induce a splitting of energy $\Delta = \Delta^{\rm ph} + \Delta^{\rm ch}$. Here the sphere indicates the location of a hole (Mn^{4+}-ion) adjacent to a Mn^{3+}-ion.

quasiparticle weight $a_{\bar{q}}$: [51]

$$a_{\bar{q}} = \begin{cases} 1 - \dfrac{1}{\sqrt{2\pi^2}} \left(\dfrac{t}{J}\right)^{1/2} & for J \gg t, \\ \sqrt[4]{2\pi^2} \left(\dfrac{J}{t}\right)^{1/4} & for J \ll t. \end{cases} \tag{1.12}$$

In the limit $J/t \to \infty$ a coherent hole motion with $a_{\bar{q}} = 1$ is recovered. In contrast to the spin $t-J$ problem in cuprates, the hole mobility in this limit is still possible due to the presence a small but finite non-diagonal hopping matrix elements which do not conserve orbital pseudospin, see Fig 1.8. Therefore the "string" effect [71] that occurs in the spin model, is less severe in the orbital $t-J$ model. In the opposite limit $J/t \to 0$, however, the holon quasiparticle weight is completely lost, which indicates a strong scattering of holes on orbital fluctuations, and the excitation spectrum of a doped hole shows only a broad continuum in a momentum space. On general grounds, it is also expected that mobile holes will fill in the orbiton gap, and will eventually destroy orbital order in a similar way as they melt spin order in cuprates.

It turns out, however, that the spatial anisotropy of e_g-orbitals provides yet another, very important channel of orbital-charge coupling which is very specific to the case of manganites. Notice that, different from the cuprates, holes remain localized up to rather high doping levels, and at the same time induce an isotropic ferromagnetic state. The complete breakdown of metalicity at hole concentrations below $x_{\rm crit} \approx 0.15$

- 0.2 occurs despite the fact that ferromagnetism is fully sustained, and is sometimes even stronger, in this regime [12, 72], which seems very surprising from the point of view a standard double-exchange picture. To explain this puzzle, the concept of orbital polarons was introduced in Ref. [51] and used for the low-doped manganites in [34, 35]. We discussed the orbital polaron concept in Section 2.1 for the purpose of describing possible orbital and charge ordering at fractional dopant concentrations, in the low doping regime. Here we treat this topic on a somewhat more theoretical level, also because orbital polaron formation can be viewed as a precursor for the orbital liquid state –these are competing states– that can occur in optimally doped manganites, which we discuss in the following Section.

The important point is that in an orbitally degenerate Mott-Hubbard system there also exists a specific coupling between holes and orbitals that stems from the polarization of e_g-orbitals in the neighborhood of a hole. In this way the cubic symmetry at manganese ions close to the hole is lifted, see Fig. 1.9). The displacement of oxygen ions, the Coulomb force exerted by the positively charged hole and hybridization of electrons cause a splitting of orbital levels. This splitting is comparable in magnitude to the kinetic energy of holes so that the orbital-hole binding energy can be large enough for holes and surrounding orbitals to form a bound state. For a given bond along the z direction the interaction reads as $H^z = -\frac{1}{2}\Delta\ n_i^h \sigma_j^z$. This is precisely the new orbital-charge coupling channel which is of course absent in pure spin-charge models. The splitting of e_g-levels effects all six sites surrounding a hole, and the analogous expressions for x and y directions can easily be derived by a rotation of the interaction Hamiltonian in orbital space. The complete orbital-charge coupling Hamiltonian for the cubic system is then

$$H_{\mathrm{ch-orb}} = -\Delta \sum_{\langle ij\rangle_\gamma} n_i^h T_j^{(\gamma)}, \tag{1.13}$$

with orbital pseudospin operators given by Eq. (1.9). The interactions in Hamiltonian (1.13) describe the tendency of the system to form orbital polarons. For low enough hole concentrations the polaron consist of a bound state between a central hole with surrounding e_g-orbitals pointing towards the hole as is shown in Fig. 1.10.

The structure of the orbital polaron yields a large amplitude of virtual excursions of e_g-electrons onto the empty site. Thus, besides minimizing the interaction energy of Hamiltonian (1.13), the polaron also allows for a lower kinetic energy. We note that these virtual hopping processes locally enhance the magnetic moments of core and e_g-spins via the double-exchange mechanism in all three directions and provide

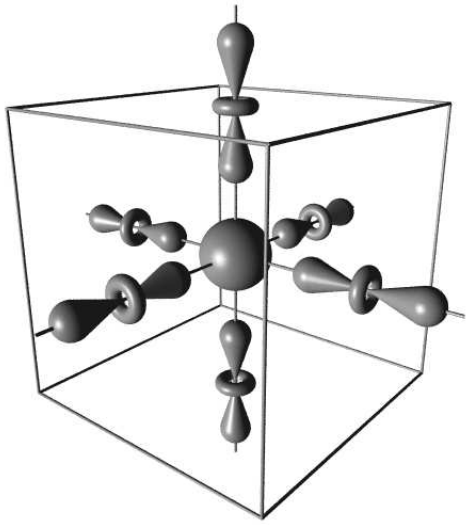

Figure 1.10. Orbital polaron in the strong-coupling limit: Six e_g- states point towards a central hole [51].

a large effective spin of the orbital polaron. This naturally explains the development of ferromagnetic clusters experimentally observed at temperatures above T_C at low doping levels [73]. At finite hole densities these clusters start to interact, thereby inducing a global ferromagnetic state. Clearly, the orbital state of such a ferromagnetic insulator must be very complex due to the presence of frozen-in orbital polarons. The relevant model must contain the interactions given by both Eqs. (1.13) and (1.10) in a first step, and further be complemented by, at least, the Coulomb forces between holes. It was suggested [51] that a such state may have orbital/Jahn-Teller glass features, which reduces the long-range component of static Jahn-Teller distortions. The orbital excitations are expected therefore to have a large broadening in a momentum space. These issues clearly deserve more theoretical work, particularly in the perspective of recent experimental results on the observation of orbital excitations in manganites [47], which hopefully can be extented to the lightly doped ferromagnetic insulator regime.

The formation of an orbital polarons competes with kinetic energy of holes that tends to delocalize the charge carriers, but also competes with the fluctuation rate $\propto xt$ of orbitals: the faster the orbitals fluctuate, the less favorable it is to form a bound state in which orbitals have to give up part of their fluctuation energy. In other words, the binding energy of

the polaron decreases at higher doping levels. When this orbital polaron picture is combined with that of conventional lattice polarons [74, 75], the transition from ferromagnetic metal to ferromagnetic insulator can be well explained [51].

Once the orbital polaron is formed it will be trapped by even a weak disorder. Near commensurate fillings, say about 1/8, they may form a polaron superlattice, optimizing simultaneously the charge and orbital configuration energies, as we discussed in section 2.1. Commensuration through phase separation –which is certainly relevant in manganites [76]– is also possible, but we will not review this complex issue here.

3.4. Orbital liquids, anomalous transport

An almost universal feature of manganites is that at higher doping concentrations (around $x \approx 1/3$) a ferromagnetic metallic state emerges. In this section we discuss the orbital state and orbital fluctuations in this regime. The appearance of a ferromagnetic metallic state is explained in a framework of double exchange physics [13, 77, 78, 79]. But if one takes the double exchange model as the starting point to explain the properties of the metallic state, it is quite surprising that in experiment one finds that the e_g-electrons do not behave as conventional spin-polarized carriers in a uniform ferromagnetic phase at all. For such carriers one expects that optical spectral weight is accumulated into a low-frequency Drude peak, but the weight of optical spectra in manganites robustly extends up to $\sim$ 1eV, even at very low temperatures [80].

This experimental finding is remarkable for at least two reasons. First, the energy scale extends to the electron-volt range, which rules out a purely phononic origin of the incoherence; and second, the incoherent spectral weight is very large in magnitude, even at low temperatures.

Other experimental studies show that collective as well as local lattice distortions are absent in metallic manganites at low temperature, which may be an indication that orbital fluctuations are strong. Based upon this observation, several authors [38, 81] attributed the incoherent structure of the optical conductivity to the orbital degrees of freedom. While the study [81] is based on a simple band picture, a more elaborate treatment of both orbital degeneracy and on-site correlations was suggested in Ref. [38]. In this work the notion of an orbital liquid, which describes a quantum disordered state of e_g-quadrupole moments in metallic manganites, was introduced. Such quantum disorder of orbitals is caused by the motion of holes which mixes up dynamically all possible orbital configurations.

At first glance this idea seems to be very similar to the concept of the moving holes that cause spin disorder in cuprates. There are two differences, however. The first one is that in a ferromagnetic system the orbital superexchange interactions are rather frustrated from the very beginning and this actually favors the orbital liquid, as we discussed previously. The effective two-dimensionality of the pseudospin fluctuations is, in fact, emphasized in [38] as an important disorder mechanism. While indeed enhancing quantum effects, this effect alone would still not be sufficient to destroy the pseudospin order, as one can see from the behavior of orbital models discussed above. Rather, it acts cooperatively with the frustrations induced by charge motion. The second, and most important, difference from cuprates is the strong tendency for holes in manganites to localize and form orbital/lattice polarons. It is the restricted charge mobility that confines the orbital liquid metallic state of manganites to a rather small region of the phase diagram.

The optical conductivity in the metallic phase of manganites has been calculated in Ref. [82], taking the idea of an orbital liquid as a starting point. The strongly correlated nature of the e_g-electrons in the metallic system can conveniently be accounted for by employing a slave-boson representation of electron operators:

$$c^{\dagger}_{i\alpha} = f^{\dagger}_{i\alpha} b_i.$$

Here the orbital pseudospin is carried by fermionic orbitons $f_{i\alpha}$, and charge by bosonic holons b_i. In comparison with other treatments of the orbital $t-J$ model [38, 70], this representation is most adapted to describe the correlated Fermi-liquid state of manganites since it naturally captures both the coherent and incoherent features of excitations. The small Drude peak as well as a broad optical absorption spectrum, that extends up to the bare bandwidth, are well reproduced by these calculations. The physical picture is that the charge carriers scatter strongly on the dynamical disorder caused by the fluctuations of orbital bonds that are due to the correlated rotation of orbitals. The fact that the anomalous transport properties in the ferromagnetic metallic phase can be described consistently, supports the validity of the orbital-liquid framework.

3.5. Fluctuating bonds, magnon anomalies

Finally, we discuss one more interesting manifestation of the orbital fluctuations in ferromagnetic metallic manganites. According to the conventional theory of double exchange, the spin dynamics of the ferromagnetic state is expected to be of nearest-neighbor Heisenberg type with a simple cosine-like magnon dispersion [83]. This picture seems indeed to

be reasonably accurate for manganese oxides with high Curie temperature T_C, i.e., for compounds with a ferromagnetic metallic phase that is sustained up to rather high temperatures [84]. Recent experimental studies on compounds with low values of T_C indicate, however, marked deviations from this canonical behavior. Quite prominent in this respect are measurements of the spin dynamics of the ferromagnetic manganese oxide $Pr_{0.63}Sr_{0.37}MnO_3$ [85]. While the spin excitation spectra exhibit conventional Heisenberg behavior at small momenta, the dispersion of magnetic excitations (magnons) shows a curious softening at the boundary of the Brillouin zone in the [1,0,0] and [1,1,0] direction but *not* in the [1,1,1] direction. The origin of this unusual softening has been attributed in Ref.[86] to the low-energy orbital fluctuations present in a "narrow-band" manganites. Let us briefly explain the basic idea. The strength of the ferromagnetic interaction at a given bond strongly depends on the orbital state of e_g-electrons (see Fig. 1.11). Along the z direction, for instance, only electrons in $d_{3z^2-r^2}$ orbitals can hop between sites and hence can participate in the double-exchange processes, but the transfer of $d_{x^2-y^2}$ electrons is blocked due to the vanishing overlap with O-2p orbitals located in-between two neighboring Mn sites. Temporal fluctuations of e_g-orbitals may thus modulate the magnetic exchange bonds, thereby renormalizing the magnon dispersion. Actually, such an effect is a quite general property of orbitally degenerate systems; the same kind of zone-boundary softening has been predicted in the insulating Kugel-Khomskii model as well [45, 58, 87].

Short-wavelength magnons are most sensitive to these local fluctuations and are affected most strongly. Quantitatively the modulation of exchange bonds is controlled by the characteristic time scale of orbital fluctuations: if the typical frequency of orbital fluctuations is higher than the timescale for spin fluctuations, the magnon spectrum remains mostly unrenormalized. In this case the orbital state effectively enters the spin dynamics only as a time average, which restores the cubic symmetry of exchange bonds. On the other hand, if orbitals fluctuate slower than spins, then the renormalization of the magnon spectrum is most pronounced and the anisotropy imposed upon the magnetic exchange bonds by the orbital degree of freedom comes into play. Also a damping of magnons is then expected to occur, which may explain the large broadening of magnons at the zone boundary.

We note that the magnons in $[1, 1, 1]$ direction are sensitive to all three spatial directions of the exchange bonds; their dispersion therefore remains unaffected by the local dynamical symmetry breaking induced by low-dimensional orbital correlations. This leads to a strong anisotropy of magnon renormalization effects in a momentum space: the $[1, 0, 0]$,

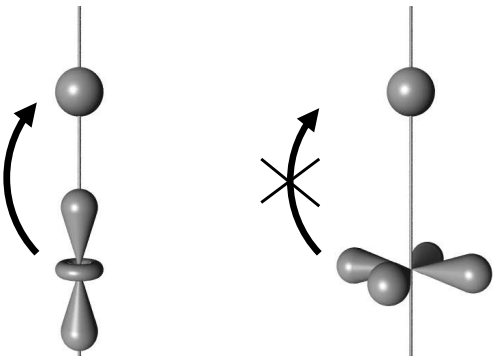

Figure 1.11. The e_g-electron transfer amplitude, which controls the double-exchange interaction $J_{\rm DE}$, strongly depends on the orbital orientation: along the z direction, e.g., $d_{3z^2-r^2}$ electrons (left) can hop into empty sites denoted by a sphere, while the transfer of $d_{x^2-y^2}$ electrons (right) is forbidden [86].

$[1, 1, 0]$ directions are mostly affected, which is actually in agreement with experiment [85]. The momentum and energy dependence of magnon anomalies are in general very sensitive to the character of local orbital correlations, and may therefore change with the evolution of underlying orbital states. In other words, if the [0,0,1] magnon mode softens to zero at the zone boundary, than this would signal the transition from ferromagnetic to the A-type antiferromagnetic spin ordering.

The unusual magnon dispersion experimentally observed in low-T_C manganites can hence be understood as a precursor effect of orbital/lattice ordering. While the softening of magnons at the zone boundary is responsible for reducing the value of T_C, the small-momentum spin dynamics that enters the spin-wave stiffness D remains essentially unaffected. This explains the enhancement of the ratio D/T_C observed in low-T_C compounds [88].

3.6. Summarizing remarks

We can state in general that quantum fluctuations of orbital degrees of freedom in manganites are important and have to be taken into account in the explanation of various properties of these systems. Despite (or even due to) the absence of the rotational symmetry in the orbital sector, profound non-classical behavior of orbitals can be caused by the

frustrating nature of interactions in the orbital sector and by the strong coupling of orbitals to doped holes.

We did not discuss the consequences of electron-phonon coupling on the orbital liquid state, so the question arises how phonons would change the physics we discussed in this section. Breathing phonons, which are certainly important for a charge localization, are actually implemented in the above picture through the interaction in Eq. (1.13). In general we expect that the coupling of the orbitals to Jahn-Teller phonons cooperates with the superexchange process in establishing orbital order and local orbital correlations. However, the fact that Jahn-Teller phonon frequencies may fall into the region of electronic orbiton energies makes the problem very difficult to analyze, particularly at the proximity to the insulator-metal transition (which is, simultaneously, an orbital solid-liquid transitions) in the phase diagram of manganites.

4. Orbital order for $x \geq 1/2$

In the phase diagram of the manganites (Fig. 1.1) there is an apparent asymmetry between the case $x < 1/2$ and the case $x > 1/2$. At lower doping levels ferromagnetic states dominate, one of which is metallic, and for high doping concentrations antiferromagnetic insulating phases dominate. Exactly at $x = 1/2$ for most manganites a rather remarkable antiferromagnetic (CE-type) charge-ordered insulating state is usually realized. In section 4.2 we discuss the properties of manganites at high doping levels and why they are so different from the systems with less doped carriers. In the next section we describe the situation at half filling and discuss the actual mechanism that leads to the CE-type (charge, orbital and magnetic) ordering in half-doped manganites.

4.1. Half-doped manganites

The half-doped manganites with $x = 1/2$ are very particular. Magnetically these systems form ferromagnetic zig-zag chains that are coupled antiferromagnetically (see Fig. 1.3 and Fig. 1.12) at low temperatures, the so-called magnetic CE-phase [8]. The ground state is, moreover, an orbitally ordered and charge-ordered insulator. This behavior is generic and is experimentally observed in $Nd_{1/2}Sr_{1/2}MnO_3$ [89, 90], $Pr_{1/2}Ca_{1/2}MnO_3$ [91], $La_{1/2}Ca_{1/2}MnO_3$ [92, 93], $Nd_{1/2}Ca_{1/2}MnO_3$ [94] and in the half-doped layered manganite $La_{1/2}Sr_{3/2}MnO_4$ [95]. The insulating charge-ordered state can be transformed into a metallic FM state by application of an external magnetic field, a transition that is accompanied by a change in resistivity of several orders of magnitude [89, 96].

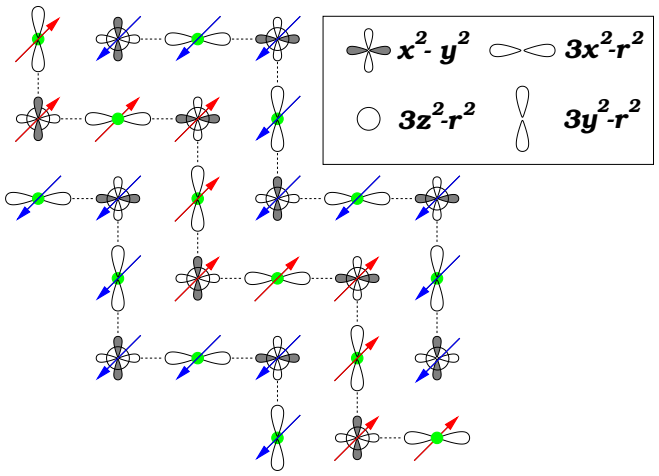

Figure 1.12. Detailed view of the CE-phase in the x-y plane. We choose our basis orbitals such that the gray lobes of the shown orbitals have a negative sign. The dots at the bridge-sites represent a charge-surplus.

The extraordinary properties of the half-doped manganites are due to the commensurability of the doping level. The disorder caused by orbital fluctuations can be quenched by magnetic, lattice and charge instabilities that are most pronounced at this commensurate filling. The combining effect of these three instabilities leads to an effectively one-dimensional insulating state, to the charge ordering and to the unusual magnetic ordering in these systems.

In the double-exchange framework electrons can only hop between sites with FM aligned core-spins so that in the CE-phase only hopping processes within the zig-zag chains are possible, rendering the system effectively one-dimensional for low-energy charge fluctuations [97, 98]. The unit cell of the quasi-1D system contains two Mn atoms, one situated at a corner site and one situated at a bridge-site, between two corners. As there are two orbitals per site, the cell has in total four different orbitals, and at half doping we have on average one electron per unit cell. The topology of the electron hopping integrals between orbitals is shown in Fig. 1.13. The important observation is that an electron that hops from one bridge-site to another bridge-site via a $|x^2-y^2\rangle$ corner-orbital obtains a phase-factor -1, while if the hopping takes place via a $|3z^2-r^2\rangle$ corner-orbital, the phase-factor is $+1$. This phase factor can be viewed as an effective dimerization that splits the four bands. These bands are shown in Fig. 1.13, where there are two bands with energy $\epsilon_\pm = \pm t\sqrt{2+\cos k}$, where k is the wave vector, and degenerate two dispersionless bands at

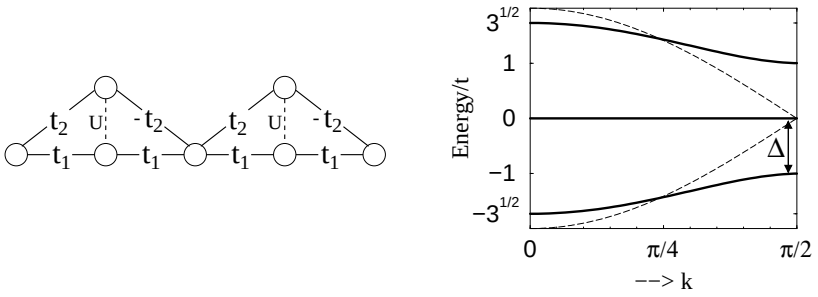

Figure 1.13. Left: Topology of the interactions in a zig-zag chain, where $t_1 = t/2$, $t_2 = t\sqrt{3}/2$, and U is the Coulomb interaction between electrons on the same site. Right: electron dispersion in the zig-zag chain of the CE-phase for $U = 0$ (solid lines) and electron dispersion in a straight chain, as in C-phase (dashed lines).

zero energy. At $x = \frac{1}{2}$ the ϵ_- band is fully occupied, and all other bands are empty. The system is insulating as the occupied and empty bands are split by a gap $\Delta = t$ and the minority bands with spin opposite to the ferromagnetic orientation of the chain (not shown) are about J_H higher in energy (J_H is the Hund's rule exchange energy). The gap is very robust as it is a consequence of the staggered phase-factor that itself is fully determined by the topology of the system. In principle other quasi 1D magnetic states, e.g. antiferromagnetically coupled ferromagnetic straight chains, are also possible; they would correspond to a state with all orbitals of the Mn-sites e.g. of the $3x^2-r^2$ type, instead of alternating $3x^2 - r^2$ and $3y^2 - r^2$ orbitals. But the presence of a gap stabilizes the CE-phase. This mechanism is equivalent to the situation in the lattice-Peierls problem, where the opening of a gap stabilizes a ground state with a lattice deformation. An extra reason for the stability of this phase maybe be the elastic interactions [27, 28]. We see the importance of the commensurability: for $x > 1/2$ the excess holes deplete the valence band, reducing the effect of the energy gain due to the gap. One expects that in this case other magnetic phases, that do not support such a gap, compete strongly with the CE-phase. If on the other hand $x < 1/2$, the excess electrons will enter in non-dispersive bands and would not contribute to the kinetic energy of the system and would thereby effectively destabilize the CE-phase. In fact it was argued that in this case the system is phase separated [98, 99, 100]. This agrees with the fact that the CE-phase survives in $Pr_{1-x}Ca_xMnO_3$ to $x = 0.3$.

But why should the system organize itself into a quasi one-dimensional state in the first place? It is rather obvious that in a three-dimensional

state, where there is much more freedom for an electron to move around, the kinetic energy would be lower. The answer is that in the manganites there are two competing magnetic interactions: the double exchange, favoring ferromagnetism, and the superexchange, that is a driving force for antiferromagnetism. The system can gain energy from both interactions simultaneously when in some direction antiferro. bonds are formed, and in other directions –ferro. bonds. Electrons can then only propagate along ferromagnetic bonds because of the double exchange. This mechanism is especially effective for systems with e_g-orbitals and is in fact quite common in the highly doped manganites –we will discuss this in the next section. The situation reminds us of the order from disorder scenario in spin-orbital models discussed in section 3.1: by forming different kinds of bonds –which is quite natural for spatially strongly anisotropic e_g-orbitals– the system gains energy.

In the CE-phase only the elongated orbitals at the bridge site (the $3x^2 - r^2$ and $3y^2 - r^2$ ones) are occupied (see Fig. 1.12). The reason is that because of the symmetry the orthogonal, planar orbitals on the bridge sites do not have any overlap with orbitals at the corner sites and in first approximation do not interact with the rest of the system. On the corner sites both orbitals are in principle partially occupied. The different orbital occupation on bridge and corner site –the orbital order– causes a lattice deformation via the Jahn-Teller coupling, thereby lowering the energy of the system still further.

Let us now discuss the consequences of electron-electron interactions at half filling. In principle one expect that short range electronic density-density interactions, that lead to the Mott insulator at zero doping, have less impact on physical properties when doping is increased, simply because the density of electrons becomes smaller and the electrons do not encounter each other very often.

As we pointed out above, the CE-phase is orbitally ordered, but charge is homogeneously distributed between corner and bridge sites if Coulomb interactions are neglected. It is well known that longer-range Coulomb interactions (for instance a nearest neighbor interaction) can cause charge ordering, especially at commensurate filling. A surprising observation, however, is that the experimentally observed charge order can be directly obtained from the degenerate double-exchange model when only the Coulomb interaction (the Hubbard U) between electrons in different orbitals, but *on the same site* is included [98]. This can be understood from the fact that in the band picture on the corner sites both orthogonal orbitals are partially occupied, but on the bridge sites only one orbital is partially filled. The on-site Coulomb interaction acts therefore differently on the corner and bridge sites: charge is pushed

away from the effectively correlated corner sites to the effectively uncorrelated bridge-sites.

The on-site Hubbard U thus leads to intersite charge disproportionation. Long-range Coulomb interactions will of course strengthen this charge ordering, and the Jahn-Teller distortion, which lowers the on-site energy of the bridge orbital with respect to the corners, also contributes to the ordering. Whereas the effect of U is to increase the ground state energy with respect to the C-phase [101] (which is made up of straight ferromagnetic chains), the longer-range Coulomb interactions will stabilize the CE-phase. This indicates that there are several competing kinetic, potential and lattice contributions to the total energy and that one needs to consider these in detail to determine the actual phase diagram [102].

4.2. Overdoped manganites

Now we qualitatively discuss the role of orbital degrees of freedom in the overdoped regime, $x > 0.5$. The main question is why the conventional double exchange, apparently responsible for the formation of the ferromagnetic metallic state for $x \sim 0.3$ – 0.4, does not lead to such a state in this case.

One reason may be the following. Usually we ascribe ferromagnetism in doped systems to a tendency to gain kinetic energy by maximal delocalization of doped charge carriers. These carriers are holes in lightly doped manganites $x < 1$, and electrons when we start e.g. from $CaMnO_3$ and substitute part of Ca by La or other rare earths, which corresponds to $x < 1$ in $La_{1-x}Ca_xMnO_3$.

There exist an important difference between these two cases, however. When we dope $LaMnO_3$, the orbital degeneracy in the ground state is already lifted by orbital ordering, and in a first approximation we can consider the motion of doped holes in a nondegenerate band. Then all the standard treatment, e.g. that of de Gennes [13], applies, and we get the FM state. However, when we start from the cubic $CaMnO_3$, we put extra electrons into empty *degenerate* e_g-levels, which form degenerate bands. Therefore we have to generalize the conventional double-exchange model to the case of degenerate bands. This was done in [18], and the outcome is the following: at relatively low electron concentration ($x \simeq 1$) the anisotropic magnetic structures –C-type (chain-like) or A-type (ferromagnetic planes stacked antiferromagnetically)– are stabilized, and only close to $x \sim 0.5$ we reach the ferromagnetic state. The C-phase occupies larger part of the phase space. The resulting theoretical phase diagram [18] is in surprisingly good agreement with the

properties of $Nd_{1-x}Sr_x$ MnO_3 [103] in which there exist the A-type "bad metal" phase for $0.52 < x < 0.65$ and C-phase for $x > 0.65$.

A simple qualitative explanation of this tendency is the following. When we start from $CaMnO_3$ with Mn^{4+} (t_{2g}^3)-ions and dope it by electrons, we put electrons into e_g-bands. The maximum energy we can gain is to put these electrons at the bottom of corresponding bands, so that one has to make these bands as broad as possible. But due to a specific character of the overlap of different e_g-orbitals in different directions, the bottom of the bands coincides for different types of orbitals: one can easily check that if we make all the orbitals e.g. $3z^2 - r^2$, the energy $\epsilon(k)$ at the Γ-point $k = 0$ will be the same as for the bands made of $(x^2 - y^2)$-orbitals. (Actually it is a consequence of the degeneracy of e_g-orbitals in cubic crystals: the symmetry at the Γ-point should coincide with the point symmetry of local orbitals, i.e. at $k = 0$ the energies of the $3z^2 - r^2$-band and of the $(x^2 - y^2)$ one, or of a band made of any linear combinations thereof of the type (1), should coincide.)

But according to the double-exchange model electrons can move only if localized moments (t_{2g}-spins) of the corresponding sites are ordered ferromagnetically (although without doping, in $CaMnO_3$ ($x = 1$), the magnetic ordering is antiferromagnetic (G-type)). Now, if we make the band e.g. out of $(x^2 - y^2)$-orbitals, the band dispersion would have the form

$$\epsilon(\vec{k}) = -2t(\cos k_x + \cos k_y) \tag{1.14}$$

i.e. the electrons in this band move only in the xy-plane, but there is no dispersion in the z-direction. Therefore to gain full kinetic energy it is enough to make this plane ferromagnetic, and the adjacent planes may well remain antiparallel to the first one. But this is just the A-type magnetic structure (ferromagnetic planes stacked antiferromagnetically). In this state we gain the same energy as in a fully ferromagnetic state (because the position of the bottom of the band is the same), but lose less exchange energy of localized t_{2g}-electrons, because two out of six bonds for each Mn are still antiferromagnetic. The same applies also to the C-type ordering, where four out of six bonds are antiferromagnetic. This explains why in the case of double exchange via degenerate orbitals –realized in overdoped manganites– predominantly these partly ferromagnetic (A-type and C-type) occur instead of full ferromagnetic ordering.

Note that in this case the electron occupy predominantly $(x^2 - y^2)$-states (or $3z^2 - r^2$-states in case of C-type ordering). Accordingly there will be a corresponding lattice distortion (compression along c-axis, $c/a < 1$, for the A-type structure, and $c/a > 1$ for the C-type one). But we want to stress that these are, strictly speaking, not the localized

orbitals, but rather the *bands* of corresponding character. Whether we should call it orbital ordering, is a matter of convention (usually this terminology is applied to the case of localized orbitals). In any case, the feature mentioned above ([22, 23]), that due to higher-order effects, in particular lattice anharmonicity, only locally elongated MeO_6-octahedra are observed in practice, is valid only for orbital ordering of *localized* orbitals, and it is in general not true for the band situation considered here.

Thus the double exchange via degenerate orbitals may quite naturally lead to anisotropic magnetic structures (A-type or C-type): we gain by that the full kinetic energy without being forced to sacrifice all the exchange interaction of localized electrons (part of the bonds remain antiferromagnetic). Which particular state will be stable at which part of the phase diagram, is determined by the competition between these terms, kinetic energy versus exchange energy, with the electron energy depending on the band filling and sensitive to the density of states for the corresponding band.

There are several factors which can complicate this picture. Thus, one may in principle get in this case canted states, and not the fully saturated A- or C-type structures [18, 104]. There may also appear inhomogeneous phase-separated states. The possibility of the charge ordering (e.g. in the form of stripes) was also not considered in [18]. But altogether it shows that the conventional double-exchange picture should be modified if double-exchange goes via degenerate orbitals, and the overall tendency which results due to this is that not the simple ferromagnetic state, but more complicated magnetic structures may be stabilized, which agrees with the general tendency observed in experiment. This factor may be important in explaining the strong qualitative asymmetry of the phase diagram of manganites for $x < 0.5$ (underdoped) and $x > 0.5$ (overdoped) regimes.

It is very interesting that stripes (and possibly bistripes) were observed in overdoped manganites [14, 15], notably in $La_{1-x}Ca_xMnO_3$ for $x = \frac{2}{3}$ and $x = \frac{3}{4}$. Orbital degrees of freedom seem to play an important role in their formation as well. The structure of the stripe and bistripe phases, see Fig. 1.14, resembles somewhat that of the CE-phase at $x = 1/2$.

The physical mechanism of the stripe formation in manganites could in principle be similar to that involved in the cuprates [105], i.e. coupling between charge and spin degrees of freedom. In manganites, however, stripes are usually formed at temperatures above those of magnetic ordering. As we see from Fig. 1.14, stripes in this case also imply a specific orbital ordering. We may think that orbital degrees of freedom and the

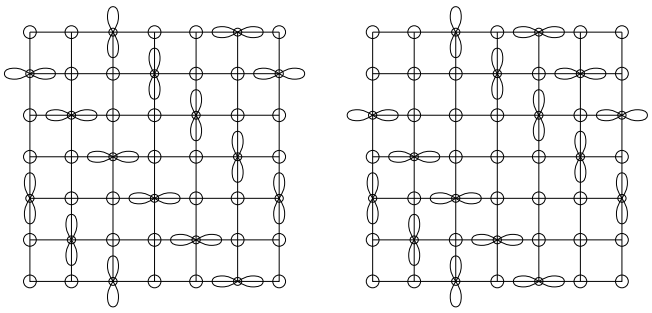

Figure 1.14. Left: single stripes ("Wigner crystal"). Right: paired stripes, or bistripes in $La_{1-x}Ca_xMnO_3$ for $x = \frac{2}{3}$. Mn^{4+} ions denoted by O and Mn^{3+} ions by 8, ∞.

corresponding lattice distortions strongly contribute to the very formation of stripes. One can indeed show that the states with a particular orbital orientation attract another, which can provide a mechanism for stripe formation [28]. As a result, depending on the values of parameters, both the single and paired stripe phases may be stabilized in overdoped manganites due to this effect [27] that heavily relies on the presence of orbital degrees of freedom.

5. Conclusions

In conclusion we can only repeat that orbital effects play a very important role in the physics of manganites, and also in many other transition metal oxides. Together with charge and spin degrees of freedom they determine all the rich variety of the properties of manganites in different doping regions. Orbital effects also play a very important role in disordered phases, determining to a large extent their transport and other properties.

An important recent achievement in this field is the development of a method to directly study orbital ordering using resonant X-ray scattering [106]. This method was successfully applied to a number of problems in manganites [12, 10, 107, 108] as well as to several other systems. And although there is still a controversy as to the detailed microscopic explanation of these observations [109, 110, 111, 112], this method will be definitely of great use in the future.

Another interesting new development is the observation of orbital excitations in $LaMnO_3$. And although many questions here still remain unclear, the recent experimental progress will definitely open a new chapter in the study of orbital effects in oxides, in particular in manganites.

In our review we left out several effects for which orbital degrees of freedom also may play an important role, e.g. phase separation [113] or short-range correlations above the ferromagnetic ordering temperature [114, 115, 116]. All these problems are now under active investigation, and the results will definitively shed new light on the physics of manganites, including the phenomenon of colossal magneto-resistance. In summary, we see that the field of orbital physics is still capable of producing important new results, and sometimes –surprises.

6. Acknowledgments

The authors gratefully acknowledge the collaboration with L.F. Feiner, P. Horsch, R. Kilian, K. Kugel, M. Mostovoy, A. M. Oleś, and G.A. Sawatzky and we also thank them for fruitful discussions.

References

[1] J. B. Goodenough, Magnetism and Chemical Bond, Interscience Publ., New York–London, 1963

[2] K. I. Kugel and D. I. Khomskii, Sov. Phys. Usp. **25**, 231 (1982).

[3] Y. Tokura and N. Nagaosa, Science **288**, 462 (2000).

[4] A. M. Oleś, M. Cuoco and N. B. Perkins, in *Lectures on the Physics of Highly Correlated Electron Systems IV*, ed. F. Mancini, AIP Conf. Proc. No. 527 (AIP, New York, 2000).

[5] H. J. Jahn and E. Teller, Proc. Roy. Soc. A**161**, 220 (1937).

[6] D. Khomskii and G. Sawatzky, Solid State Comm. **102**, 87 (1997).

[7] D. Khomskii, "Electronic structure, exchange and magnetism in oxides", in *Spin Electronics* p. 89, eds. M. Ziese and M.J. Thornton, Springer Verlag (2001).

[8] E. O. Wollan and W. C. Koehler, Phys. Rev. **100**, 545 (1955).

[9] Z. Jirak *et al.*, J. Magn. Magn. Mater. **53**, 153 (1985).

[10] M. v. Zimmermann *et al.*, Phys. Rev. Lett. **83**, 4872 (1999).

[11] T. Niemöller et al, Eur. Phys. J. **B8**, 5 (1999); R. Klingerer *et al.*, preprint (2001).

[12] Y. Endoh, K. Hirota, S. Ishihara, S. Okamoto, Y. Murakami, A. Nishizawa, T. Fukuda, H. Kimura, H. Nojiri, K. Kaneko, and S. Maekawa, Phys. Rev. Lett. **82**, 4328 (1999).

[13] P. G. de Gennes, Phys. Rev. **118**, 141 (1960).

[14] P. G. Radaelli *et al.*, Phys. Rev. B **59**, 14440 (1999).

[15] S. Mori, C. H. Chen and S.-W. Cheong, Nature **392**, 479 (1998).

[16] R. Wang *et al.*, Phys. Rev. B **61**, 11946 (2000).

[17] C. Martin *et al.*, J. Solid State Chem. **134**, 198 (1997).

[18] J. van den Brink and D. Khomskii, Phys. Rev. Lett. **82**, 1016 (1999).

[19] G. A. Gehring and K. A. Gehring, Rep. Progr. Phys. **38**, 1 (1975).

[20] K. I. Kugel and D. Khomskii, JETP Lett. **15**, 446 (1972); K. I. Kugel and D. Khomskii, Sov. Phys.–JETP **37**, 725 (1973).

[21] P. W. Anderson, Phys. Rev. **115**, 2 (1959).

[22] J. Kanamori, J. Appl. Phys. (Suppl.) **31**,14S (1960).

[23] D. Khomskii and J. van den Brink, Phys. Rev. Lett. **85**, 3229 (2000).

[24] R. Englman and B. Halperin, Phys. Rev. B **2**, 75 (1970); B. Halperin and R. Englman, Phys. Rev. B **3**, 1698 (1971).

[25] J. D. Eshelby, Solid State Phys., ed. F. Seitz and D. Turnbull, Academic Press, New York, v. 3, p. 79 (1956).

[26] A. G. Khachaturyan, Theory of Phase Transformations and the Structure of Solid Solutions, Nauka, Moscow (1974).

[27] D. Khomskii and K. I. Kugel, Europhys. Lett. **55**, 208 (2001).

[28] D. Khomskii and K. I. Kugel, cond-mat/0112340 (2001).

[29] Y. Yamada *et al.*, Phys. Rev. Lett. **77**, 904 (1996).

[30] T. Inami *et al.*, Jap. J. Appl. Phys., Suppl **38-1**, 212 (1999).

[31] Y. Yamada *et al.*, Phys. Rev. B. **62**, 11600 (2000).

[32] D. Cox *et al.*, Phys. Rev. B. **64**, 024431 (2001).

[33] M. v. Zimmermann *et al.*, cond-mat/0007321 (2000).

[34] T. Mizokawa, D. Khomskii and G. Sawatzky, Phys. Rev. B **61**, R3776 (2000).

[35] T. Mizokawa, D. Khomskii and G. Sawatzky, Phys. Rev. B **63**, 024403 (2000).

[36] R. Kilian and G. Khaliullin, Phys. Rev. B **60**, 13458 (1999).

[37] D. Louca and T. Egami, J. Appl. Phys. **81**, 5484 (1997); Phys. Rev. B. **59**, 6193 (1999).

[38] S. Ishihara, M. Yamanaka and N. Nagaosa, Phys. Rev. B **56**, 6861 (1997).

[39] D. Khomskii, cond-mat/0004034 (2000).

[40] J. van den Brink and D. Khomskii, Phys. Rev. B **63**, 1401416(R), (2001).

[41] R. Maezono and N. Nagaosa, Phys. Rev. B **62**, 11576 (2000).

[42] A. Takahashi and H. Shiba, J. Phys. Soc. Jap. **69**, 3328 (2000).

[43] S. Ishihara, J. Inoue and S. Maekawa, Phys. Rev. B **55**, 8280 (1997).

[44] J. van den Brink *et al.*, Phys. Rev. B **58**, 10276 (1998).

[45] G. Khaliullin and V. Oudovenko, Phys. Rev. B **56**, R14243 (1997).

[46] J. van den Brink, Phys. Rev. Lett. **87**, 217202 (2001).

[47] E. Saitoh, S. Okamoto, K. T. Takahashi, K. Tobe, K. Yamomoto, T. Kimura, S. Ishihara, S. Maekawa, and Y. Tokura, Nature (London) **410**, 180 (2001).

[48] P.B. Allen and V. Perebeinos, Nature **410**, 155 (2001).

[49] L. F. Feiner, A. M. Oleś, and J. Zaanen, Phys. Rev. Lett. **78**, 2799 (1997).

[50] V. Perebeinos and P.B. Allen, Phys. Rev. Lett. **85**, 5178 (2000).

[51] R. Kilian and G. Khaliullin, Phys. Rev. B **60**, 13458 (1999).

[52] J. van den Brink, P. Horsch and A.M. Oleś Phys. Rev. Lett. **85**, 5174 (2000).

[53] J. B. Goodenough, Phys. Rev. **100**, 564 (1955).

[54] J. Villain *et al.*, J. Physique **41**, 1263 (1980).

[55] E.F. Shender, Sov. Phys.–JETP **56**, 178 (1982).

[56] For a discussion of the order from disorder phenomena in frustrated spin systems, see A. M. Tsvelik, *Quantum Field Theory in Condensed Matter Physics* (Cambridge University Press, Cambridge, 1995), Chap. 17, and references therein.

[57] L. F. Feiner, A. M. Oleś, and J. Zaanen, J. Phys. Condens. Matter **10**, L555 (1998).

[58] G. Khaliullin and R. Kilian, J. Phys. Condens. Matter **11**, 9757 (1999).

[59] J. van den Brink, P. Horsch, F. Mack, and A. M. Oleś, Phys. Rev. B **59**, 6795 (1999).

[60] See the discussion in Ref. [2], p.253.

[61] G. Khaliullin, Phys. Rev. B **64**, 212405 (2001).

[62] G. Khaliullin and P. Horsch, unpublished.

[63] K. Kubo, J. Phys. Soc. Jpn. 71 (2002), in press.

[64] S.J. Glass and J.O. Lawson, Phys. Lett. **A 43** 234 (1973).

[65] K.I. Kugel and D.K. Khomskii, Sov. Phys.-Solid State Phys. **17** 285 (1975).

[66] Note also the weaker orbital-lattice coupling and hence the less destructive effect of cooperative lattice distortions on orbital fluctuations in t_{2g}-systems.

[67] G. Khaliullin, and S. Maekawa, Phys. Rev. Lett. **85**, 3950 (2000).

[68] B. Keimer, D. Casa, A. Ivanov, J. W. Lynn, M.v. Zimmermann, J. P. Hill, D. Gibbs, Y. Taguchi, and Y. Tokura, Phys. Rev. Lett. **85**, 3946 (2000).

[69] G. Khaliullin, P. Horsch, and A. M. Oleś, Phys. Rev. Lett. **86**, 3879 (2001).

[70] S. Ishihara, J. Inoue, and S. Maekawa, Phys. Rev. B **55**, 8280 (1997).

[71] L.N. Bulaevskii, E.L. Nagaev and D.I. Khomskii, Sov. Phys.–JETP **27**, 836 (1968).

[72] S. Uhlenbrusk *et al.*, Phys. Rev. Lett. **82**, 185 (1999).

[73] J. M. De Teresa, M. R. Ibarra, P. A. Algarabel, C. Ritter, C. Marquina, J. Blasco, J. Garcia, A. del Moral, and Z. Arnold, Nature (London) **386**, 256 (1997).

[74] A. J. Millis, B. I. Shraiman, and R. Mueller, Phys. Rev. Lett. **77**, 175 (1996); A. J. Millis, Nature (London) **392**, 147 (1998).

[75] J. H. Röder, J. Zang, and A. R. Bishop, Phys. Rev. Lett. **76**, 1356 (1996).

[76] For a discussion of phase separation issue, see, for example, A. Moreo, S. Yunoki, and E. Dagotto, Science **283**, 2034 (1999).

[77] C. Zener, Phys. Rev. **82**, 403 (1951).

[78] P. W. Anderson and H. Hasegawa, Phys. Rev. **100**, 675 (1955).

[79] K. Kubo and N. Ohata, J. Phys. Soc. Jpn. **33**, 21 (1972).

[80] Y. Okimoto, T. Katsufuji, T. Ishikawa, A. Urushibara, T. Arima, and Y. Tokura, Phys. Rev. Lett. **75**, 109 (1995).

[81] H. Shiba, R. Shiina, and A. Takahashi, J. Phys. Soc. Jpn. **66**, 941 (1997).

[82] R. Kilian and G. Khaliullin, Phys. Rev. B **58**, R11 841 (1998).

[83] N. Furukawa, J. Phys. Soc. Jpn. **65**, 1174 (1996).

[84] T. G. Perring, G. Aeppli, S. M. Hayden, S. A. Carter, J. P. Remeika, and S.-W. Cheong, Phys. Rev. Lett. **77**, 711 (1996).

[85] H. Y. Hwang, P. Dai, S.-W. Cheong, G. Aeppli, D. A. Tennant, and H. A. Mook, Phys. Rev. Lett. **80**, 1316 (1998).

[86] G. Khaliullin and R. Kilian, Phys. Rev. B **61**, 3494 (2000).

[87] J. van den Brink, W. Stekelenburg, D.I. Khomskii, G.A. Sawatzky and K.I. Kugel, Phys. Rev. B. **58**, 10276 (1998)

[88] J. A. Fernandez-Baca, P. Dai, H. Y. Hwang, C. Kloc, and S.-W. Cheong, Phys. Rev. Lett. **80**, 4012 (1998).

[89] H. Kuwahara *et al.*, Science **270**, 961 (1995).

[90] H. Kawano *et al.*, Phys. Rev. Lett. **78**, 4253 (1997).

[91] Z. Jirac *et al.*, J. Magn. Magn. Mater. **53**, 153 (1985), Y. Tomioka *et al.*, Phys. Rev. B **53**, R1689 (1996).

[92] Y. Okimoto *et al.*, Phys. Rev. Lett. **75**, 109 (1995), P. Schiffer *et al., ibid.* **75**, 3336 (1995), P. G. Radaelli *et al., ibid.* **75**, 4488 (1995), Y. Okimoto *et al.*, Phys. Rev. B **55**, 4206 (1997).

[93] S. Mori, C.H. Chen and S.-W. Cheong, Nature **392**, 473 (1998).

[94] T. Kimura *et al.*, unpublished.

[95] Y. Moritomo *et al.*, Phys. Rev. B **51**, 3297 (1995), B.J. Sternlieb *et al.*, Phys. Rev. Lett. **76**, 2169 (1996), Y. Moritomo *et al.*, Nature **380**, 141 (1996).

[96] M. Tokunaga *et al.*, Phys. Rev. B **57**, 5259 (1998).

[97] I. V. Solovyev and K. Terakura, Phys. Rev. Lett. **83**, 2825 (1999).

[98] J. van den Brink, G. Khaliullin and D. Khomskii, Phys. Rev. Lett. **83**, 5118(1999).

[99] N.A. Babushkina *et al.*, Phys. Rev. B **59**, 6994 (1999), M. Uehara *et al.*, Nature **399**, 560 (1999).

[100] M.Y. Kagan, D.I. Khomskii and K.I. Kugel, JETP **93**, 415 (2001).

[101] S.-Q. Shen, Phys. Rev. Lett. **86**, 5842 (2001).

[102] J. van den Brink, G. Khaliullin and D. Khomskii, Phys. Rev. Lett. **86**, 5843 (2001).

[103] H. Kuwahara *et al.*, Mat. Res. Soc. Symp. Proc., v. 494, 83 (1998).

[104] I. Solovyev and K. Terakura, Phys. Rev. B in press (2001).

[105] J. Zaanen and O. Gunnarsson, Phys. Rev. B **40**, 7391 (1989).

[106] Y. Murakami *et al.*, Phys. Rev. Lett. **80**, 1932 (1998).

[107] Y. Murakami *et al.*, Phys. Rev. Lett. **81**, 582 (1998).

[108] Y. Wagabagashi *et al.*, J. Phys. Soc. Jap. **69**, 2731 (2000).

[109] S. Ishihara and S. Maekawa, Phys. Rev. Lett. **80**, 3799 (1998).

[110] I. S. Elfimov, V. A. Anisimov and G. Sawatzky, Phys. Rev. Lett. **82**, 4264 (1999).

[111] M. Benfatto *et al.*, Phys. Rev. Lett. **83**, 636 (1999).

[112] P. Benedetti, J. van den Brink, E. Pavarini, A. Vigliante, and P. Wochner, Phys. Rev. B. **63**, 60408(R) (2001).

[113] E. Dagotto, T. Hotta and A. Moreo, Phys. Rep. **344**, 1 (2001).

[114] L. Vasiliu-Doloc *et al.*, Phys. Rev. Lett. **83**, 4393 (1999).

[115] C.P. Adams *et al.*, Phys. Rev. Lett. **85**, 3954 (2000).

[116] P. Dai *et al.*, Phys. Rev. Lett. **85**, 2553 (2000).